







RESEARCH ARTICLE | JUNE 12 2023

## The nucleation, growth, and adhesion of water bridges in sliding nano-contacts

Special Collection: [Adhesion and Friction](#)

Felix Cassin   ; Rachid Hahury  ; Thibault Lançon  ; Steve Franklin  ; Bart Weber 

 Check for updates


*J. Chem. Phys.* 158, 224703 (2023)

<https://doi.org/10.1063/5.0150276>

  
View  
Online


  
Export  
Citation

CrossMark



**The Journal of Chemical Physics**  
Special Topic: Adhesion and Friction

**Submit Today!**



# The nucleation, growth, and adhesion of water bridges in sliding nano-contacts



Cite as: J. Chem. Phys. 158, 224703 (2023); doi: 10.1063/5.0150276

Submitted: 13 March 2023 • Accepted: 8 May 2023 •

Published Online: 12 June 2023



View Online



Export Citation



CrossMark

Felix Cassin,<sup>1,2,a)</sup> Rachid Hahury,<sup>1</sup> Thibault Lançon,<sup>1</sup> Steve Franklin,<sup>1,3</sup> and Bart Weber<sup>1,2</sup>

## AFFILIATIONS

<sup>1</sup>Advanced Research Center for Nanolithography (ARCNL), Science Park 106, 1098XG Amsterdam, The Netherlands

<sup>2</sup>Van der Waals-Zeeman Institute, Institute of Physics, University of Amsterdam, Science Park 904, 1098 XH Amsterdam, The Netherlands

<sup>3</sup>Department of Materials Science and Engineering, The University of Sheffield, Sheffield S1 3JD, United Kingdom

**Note:** This paper is part of the JCP Special Topic on Adhesion and Friction.

<sup>a)</sup>Author to whom correspondence should be addressed: [fec49@pitt.edu](mailto:fec49@pitt.edu)

## ABSTRACT

We provide experimental observations of the nucleation and growth of water capillary bridges in nanometer gaps between a laterally moving atomic force microscope probe and a smooth silicon wafer. We find rising nucleation rates with increasing lateral velocity and a smaller separation gap. The interplay between nucleation rate and lateral velocity is attributed to the entrainment of water molecules into the gap by the combination of lateral motion and collisions of the water molecules with the surfaces of the interface. The capillary volume of the full-grown water bridge increases with the distance between the two surfaces and can be limited by lateral shearing at high velocities. Our experimental results demonstrate a novel method to study *in situ* how water diffusion and transport impact dynamic interfaces at the nanoscale, ultimately leading to friction and adhesion forces at the macroscale.

© 2023 Author(s). All article content, except where otherwise noted, is licensed under a Creative Commons Attribution (CC BY) license (<http://creativecommons.org/licenses/by/4.0/>). <https://doi.org/10.1063/5.0150276>

## I. INTRODUCTION

The abundance of water in the atmosphere, biosphere, and lithosphere of Earth and its inherent properties and forces enable and contribute to countless natural phenomena.<sup>1</sup> When confined to small spaces between solids, water becomes one of the main drivers in processes observed in nature. This ranges from water transport from root to leaf in plants<sup>2–4</sup> to molecule transfer of nutrients or contaminants in porous soil,<sup>5,6</sup> transport of natural gas in coal- or shale-rich rocks,<sup>5,7–9</sup> volcano formation in tectonic subduction zones,<sup>10</sup> or metal ore deposit formation by hydrothermal flow of water through pores and cracks in geological formations.<sup>10</sup> The presence of water in vapor phase or as adsorbed liquid films on surfaces has also been a challenge<sup>11–13</sup> and solution<sup>14,15</sup> for engineering projects throughout history. The resulting adhesion and friction forces in sliding contacts were first mentioned by Charles-Augustin de Coulomb in his pioneering work “Theory of Simple Machines” (1821), noting the contribution of adhesion to friction as well as the growth of static friction force with increasing contact time

between two bodies.<sup>16–19</sup> Recent tribological studies emphasize the importance of water in controlling capillary adhesion, friction, and wear at silicon interfaces.<sup>14,20–25</sup> Multiple factors influence the formation, growth, size, and force of capillary bridges, such as contact size, local gap size<sup>26–28</sup> in the contact interface, contact time,<sup>29–31</sup> lateral and vertical velocities,<sup>32–36</sup> material properties (e.g., hydrophobicity<sup>37</sup> and roughness<sup>38</sup>), and environmental factors, including relative humidity,<sup>28,39–41</sup> temperature,<sup>42</sup> and pressure.<sup>43</sup>

When two surfaces are brought within a critical distance to each other, chains of water molecules with a nanoscale volume can condense from the vapor phase through Knudsen diffusion<sup>29,44</sup>—diffusion in which the mean free path is interrupted by the system walls—and form connections across the interface.<sup>27</sup> The negative Laplace pressure inside such capillary bridges, together with the surface tension, pulls the two surfaces toward each other. This attractive force induced by water capillary bridges contributes to the externally applied contact force and, therefore, impacts the load-controlled friction force.<sup>20,30,45,65</sup> Atomic Force Microscope (AFM) and tuning fork experiments<sup>42,46</sup> have shown that capil-

lary bridge nucleation is a thermally activated and, thus, stochastic process<sup>31,35,42,47</sup> that requires an average activation time. Experimentally measured activation times and energy barriers<sup>42,47,48</sup> as well as analytical predictions indicate that a freshly nucleated water bridge has a volume of just a few cubic nanometers. Subsequent to nucleation, the water bridge grows via vapor diffusion, Knudsen diffusion, and adsorbed water layer thin film flow<sup>11,29,49</sup> until a steady capillary bridge volume is reached. While previous experiments have suggested that lateral sliding plays a crucial role in the steady-state capillary bridge size and, with that, its adhesion,<sup>33</sup> it has been experimentally challenging to observe the influence of lateral velocity on the two-step process of nucleation and growth to a full-sized capillary bridge. The bridge growth following the nucleation of a capillary remains especially elusive and difficult to observe *in situ* under dynamic conditions.

We developed a novel AFM scanning technique to observe *in situ* the nucleation and growth of nanoscale capillary bridges at a laterally moving interface. We are able to reach lateral displacements of up to 5  $\mu\text{m}$  with velocities ranging from 1 to 200  $\mu\text{m/s}$  while maintaining a sub-nanometer precise gap between the AFM probe and the silicon (Si) wafer sample. We show that smaller tip-sample distances lower the activation time for capillary bridges, which then grow within 1–10 ms—at a tip-sample distance-independent rate—to their final size, which generates 1–10 nN adhesion forces. Surprisingly, the lateral motion reduces the measured activation times for capillary nucleation, which may be attributed to the interplay between gas diffusion and lateral velocity. These insights contribute to a predictive understanding of the dynamics that dictate capillary adhesion.

## II. MATERIALS AND METHODS

For the experimental observations of nucleation, growth, and steady-state adhesion behavior of water capillary bridges as a function of lateral velocity and gap size, a Bruker Innova™ Atomic Force Microscope (AFM) was used in Lift Mode. Both the probe and substrate are made from silicon, with a native oxide layer of a few nanometers on the surface. The oxidized silicon chosen as a model system is representative of single asperity contacts in, e.g., semiconductor devices. To combine a defined contact geometry with accurate control over tip-sample distance and adhesion measurements, relatively stiff AFM probes (silicon Bruker RTESPA300-30 AFM probe, tip radius  $r = 30$  nm, cantilever stiffness  $C = 38$ – $43$  N/m) formed a dynamic interface with a piece of a silicon wafer (University Wafers, test grade, rms roughness  $\sim 140$  pm,  $2 \times 0.5$   $\mu\text{m}^2$ ). We chose silicon wafer samples not only because such surfaces are important, for instance, in MEMS and NEMS technology—where capillary condensation and adhesion can deteriorate performance—but also to avoid any significant deviation from the set Lift Mode height (tip-sample distance) during higher lateral velocities. The smoother the substrate is, the easier it is for the AFM tip to follow the recorded topography with an offset at high velocity. Given that the expected range of adhesion forces for the nanoscopic tip-on-sample contact is just a few nanonewtons, the stiffness of the cantilever will result in a vertical deflection in the tens of picometer range. Thanks to the gold coating on the backside of the cantilever, this small change in deflection is still reliably detectable, while the change in the tip-sample distance due to the downward bend does

not exceed more than 0.1 nm. The Lift Mode technique, often used for magnetic, surface charge, or conductivity measurements,<sup>50,51</sup> utilizes the Z-direction (normal to the interface) piezo of the AFM scan head to impose a well-defined distance between the sample and the AFM-probe during lateral scanning. The surface topography is recorded in contact mode with a set point of  $\sim 22$  nN during the trace scan (tip moves from left to right, 100 nm to 5  $\mu\text{m}$ ). After completing the trace scan, the probe retracts from the sample surface to a separation height (tip-sample distance) of 50 nm, which will rupture any capillary bridges formed between the tip and surface during the topography scan. Afterward, the probe is lowered to a selected tip-sample distance and retraces the previously recorded topography on the same line but with the chosen Z-offset, maintaining a constant gap between the tip and the sample with sub-nanometer precision, even on surfaces with nano-roughness. Every Lift Mode measurement at a chosen velocity and tip-sample distance consists of 64–128 lines, with each line representing an individual capillary bridge formation attempt. A typical retrace scan with observable nucleation in each backward line can be seen in the inset of Fig. 1. Each line shows the activation time to nucleate a capillary bridge (yellow in the color bar). Once a bridge is formed and grows, the vertical bending of the cantilever increases quickly, and the retrace line transitions from yellow to blue in the color scale.

To investigate the influence of lateral velocity on the growth of capillary bridges, Lift Mode scans were performed with scanning velocities ranging from 0.2 to 200  $\mu\text{m/s}$  at three distinct tip-sample distances of 0.2, 0.7, and 1.2 nm. A separate set of experiments with three lateral velocities of 10, 30, and 50  $\mu\text{m/s}$  focused on the influence of separation gap distances between 0.4 and 2.0 nm. Force-distance measurements were performed at regular intervals during the experiments to check for tip wear and to calibrate the tip-sample distance. The measured adhesion forces stayed in the expected range for a 30 nm radius tip, suggesting very little negligible wear throughout the experiment set. The distance of zero was defined as the z-position at which the adhesive and repulsive forces acting on the cantilever during tip-sample contact cancel each other out and no vertical bending can be observed.<sup>42</sup> All velocity and distance measurements were performed in a randomized order. Other influential factors, such as temperature (22 °C) or humidity ( $\sim 50\%$  RH), were kept stable during experiments.

## III. RESULTS AND DISCUSSION

### A. Nucleation

The Lift Mode experiments (Fig. 1) uniquely enable recordings of the nucleation, growth, and stabilization of a water capillary bridge at the interface between the oxidized silicon AFM tip and substrate. Knowing the lateral velocity, the sliding and hovering distances measured can be converted to time. The average activation time—defined as the time the tip hovers over the substrate before a change in adhesion is detected—strongly depends on the tip-sample distance [Fig. 2(a)]. The nucleation occurs faster at smaller tip-sample distances. The nucleation of a capillary bridge is a thermally activated process with an activation energy given by<sup>42</sup>

$$\Delta E(h) = k_B T \ln(p_s/p) Ah\rho, \quad (1)$$

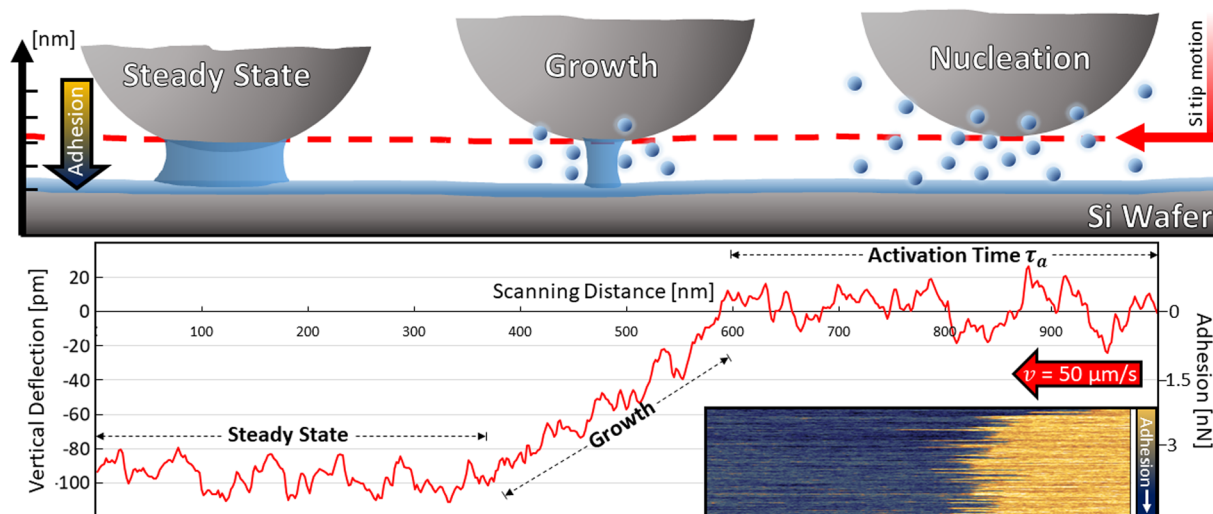


**FIG. 1.** Working principle of the Lift Mode measurements. After measuring the sample topography in contact mode during the trace, the tip is retracted and approaches the sample again. The tip then retraces the recorded topography from right to left with a defined lateral motion velocity and tip-sample distance. The schematic at the top shows the steps of capillary bridge nucleation and growth. The graph shows the recorded vertical deflection of a single retrace line (right to left) at a velocity  $v$  of  $50 \mu\text{m/s}$  with a tip-sample distance of  $0.8 \text{ nm}$ . After activation time  $\tau_a$ , water molecules from the surrounding atmosphere nucleate into a capillary bridge, which quickly grows to its steady-state size. Its capillary adhesion force bends the cantilever toward the sample surface, resulting in a measurable negative vertical deflection in the picometer range. The inset shows a typical vertical deflection retrace scan image, where each scan line represents an individual nucleation event. The vertical deflection is proportional to the adhesion force; initially, the traces show no adhesion (yellow), but as a capillary bridge nucleates and grows, so does the adhesion (blue).

where  $k_B$  is the Boltzmann constant,  $T$  is the temperature,  $(p_s/p)$  is the partial pressure of water in the environment, also referred to as the relative humidity,  $A$  is the in-plane area of the nucleated capillary bridge,  $h$  is the height (tip-sample distance) of the nucleated capillary bridge, and  $\rho$  is the number density of liquid water. The activation time required to successfully nucleate a water capillary bridge is, therefore,<sup>42</sup>

$$\tau_a(h) = \tau_0 \exp[\Delta E(h)/(k_B T)], \quad (2)$$

where  $\tau_0$  is a pre-factor that can be translated into an attempt frequency of  $1/\tau_0$  with values between 1 and 300 GHz.<sup>42,47</sup> The broad range of attempt frequencies reported in the literature indicates that a quantitative comparison between Eq. (2) and experiments remains challenging. Rather than nucleation time, the inverse nucleation time or nucleation rate ( $1/\tau_a$ ) is often reported in the literature.<sup>42,47,52</sup> In agreement with both the thermal activation model and previous experimental studies, we find an exponential increase in activation time with tip-sample distance, measuring typical activation times in the millisecond regime [Fig. 2(a)]. The key advantage of Lift Mode experiments is that, next to tip-sample distance, the tip velocity can be controlled, allowing us to address the previously unanswered question of how lateral motion influences the capillary bridge nucleation process. Contact mode AFM experiments have demonstrated that lateral velocity can, indeed, strongly impact capillary adhesion; the growth of capillary bridges is hindered above a critical sliding velocity.<sup>33</sup> Surprisingly, we observe the opposite for the nucleation of capillary bridges: the nucleation rate rather increases with rising

velocity [Fig. 2(b)]. This counterintuitive behavior is further emphasized by a second set of experiments in which the tip velocity was systematically varied for three different tip-sample distances [Fig. 2(b)].

A possible explanation for the lower activation times with increasing velocity originates in the main diffusion process<sup>39</sup> responsible for nucleation. The mean free path of water molecules in the vapor phase (130 nm in ambient conditions) is at least an order of magnitude larger than the nano-sized separation gaps in the performed experiments, resulting in Knudsen numbers—describing the ratio of the gap to the mean free path<sup>53</sup>— $K_n$  between 25 and 300. The diffusion is, therefore, mostly controlled by the collisions of molecules with the adsorbed water layers on the tip and sample surfaces.<sup>44</sup> Thus, with decreasing tip-sample distance, the Knudsen diffusion coefficient rises.<sup>34,35</sup> Water molecules diffusing toward the tip-to-sample interface are assisted by the lateral motion of the tip at the leading edge of the interface. By moving into the pathways of water molecules and additionally reducing the interface gap for the next collision (see Fig. 3, dashed lines), the induced pressure gradient is further increased, and the inward flux of water vapor rises. This may then increase the water capillary bridge nucleation rate with lateral velocity. The model calculations have indicated that the time required to Knudsen diffuse from the perimeter of an AFM tip-on-flat contact to its center is of the order of 1–100 ms, while the typical Knudsen length over which this diffusion takes place is 50 nm.<sup>54</sup> The ratio of this length to the time scale matches the experimental velocities (50–5000  $\mu\text{m/s}$ ), making an interplay between Knudsen diffusion, lateral velocity, and nucleation rate plausible (Fig. 4).

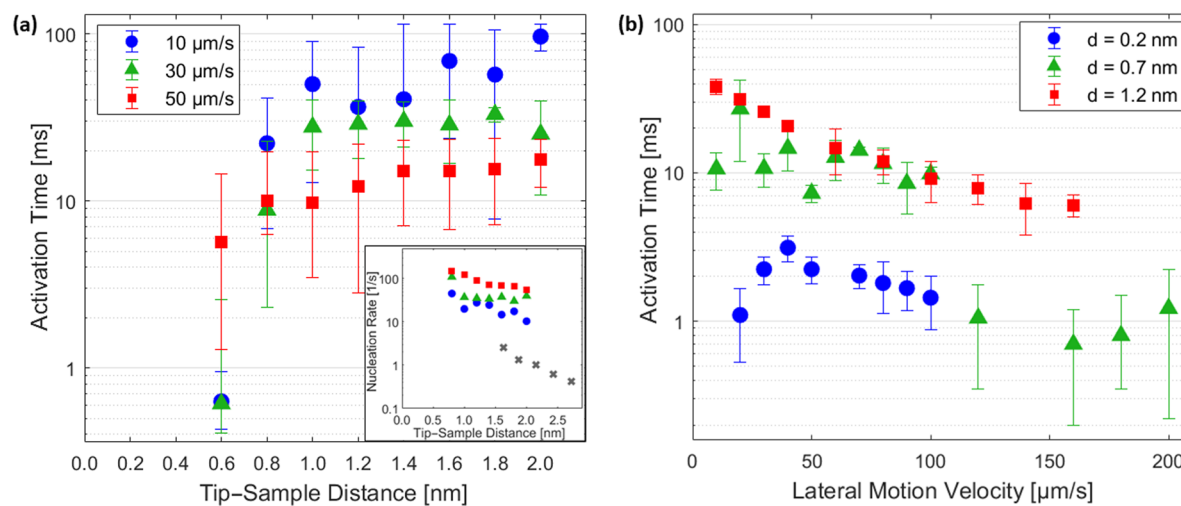


**FIG. 2.** Activation time as a function of tip-sample distance and lateral motion velocity. (a) Activation time decreases approximately exponentially with smaller distances to the sample for all three measured velocities. Inset: A comparison of the nucleation rates ( $1/\tau_a$ ) of three velocities with values from Sung *et al.*<sup>47</sup> showing the influence of lateral velocity on the nucleation process. (b) Activation times at tip-sample distances of 0.2, 0.7, and 1.2 nm with lateral motion velocities up to 200  $\mu\text{m/s}$ . The error bars reflect the standard deviation of the observed activation times.

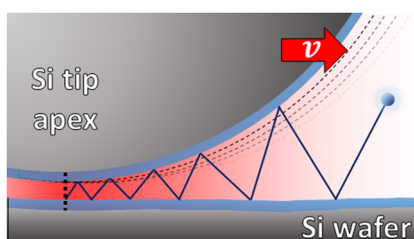


**FIG. 3.** The path of a water molecule is controlled by the collisions with the adsorbed water layers at the interface. Knudsen diffusion creates a vapor pressure difference (red gradient). By moving the probe laterally (dashed line), the diffusion of water molecules toward the apex of the tip is enhanced at the leading edge of the interface.

## B. Growth and stabilization

To understand the relative importance of the two separate processes of capillary nucleation and growth<sup>33</sup> in generating the observed adhesion forces, we further analyze the water volumes involved in the nucleation and growth processes. Based on the typical measured activation times of 1–100 ms, the capillary nucleus volume according to Eq. (1) is 0.5–2  $\text{nm}^3$ , with a capillary area  $A$  estimated to be of the order of the size of a few water molecules: 0.05–4  $\text{nm}^2$ . A rough estimate of the adhesion force generated by such a small capillary bridge can be obtained by taking the product of  $A$  and the Laplace pressure difference, which is given by the ratio of the water surface tension to the Kelvin radius. The estimated values for  $A$ , based on the measured activation times, thus translate into adhesion forces of 0.001–0.3 nN. This is small compared

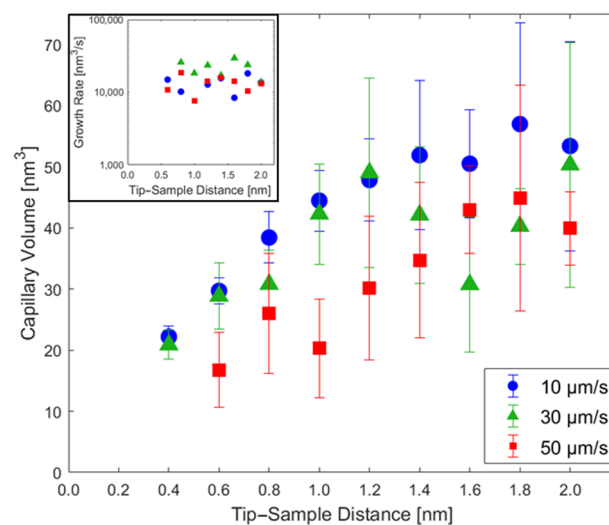


**FIG. 4.** Growth and steady-state volume of capillary bridges at different tip-sample distances. The estimated steady-state volume of capillary bridges increases approximately linearly with tip-sample distance. Inset: The growth rate for all three velocities remains stable at about 10 000  $\text{nm}^3/\text{s}$  over the measured tip-sample distances.

to the experimentally measured adhesion forces of 2–5 nN, presumably because the capillary bridge grows after nucleation.<sup>17</sup> The Lift Mode measurements uniquely reveal a time-resolved recording of meniscus growth and stabilization (Fig. 1). Furthermore, because the Lift Mode experiments reveal the adhesion force, the capillary bridge volumes can be estimated. By dividing the measured adhesion

force by the Laplace pressure, we can estimate the growing capillary area  $A$  and, together with the tip-sample distance  $d$ , the growing capillary volume:  $V_{cap} = A \cdot d$ . It should be noted that the resulting capillary volumes need to be interpreted as rough estimates. The growing capillary bridge is not in thermodynamic equilibrium, meaning that the curvature of the capillary bridge can deviate from that predicted by the Kelvin equation. The steady-state capillary volume strongly depends on the tip-sample distance (Fig. 3); at larger distances, capillary bridges of up to  $60 \text{ nm}^3$  can be grown. The time required for the growth—defined as the time during which the adhesion force transitions from 0 to its steady-state value—scales approximately linearly with the steady-state capillary bridge volume. In other words, the growth rate—defined as the estimated final capillary bridge volume divided by the growth time—is independent of the tip-sample distance (Fig. 3). This observation strongly contrasts the dynamics of capillary nucleation: The nucleation of the capillary bridge depends exponentially on the tip-sample distance. The rate at which water is added to the capillary bridge during growth is about  $7500\text{--}30\,000 \text{ nm}^3/\text{s}$ . In comparison, the volume of a freshly nucleated meniscus divided by a typical activation time is  $2 \text{ nm}^3/10 \text{ ms} = 200 \text{ nm}^3/\text{s}$ , significantly lower than the growth rate. An important factor here is the very high water adsorption rate of the growing bridge nucleated at the smallest separation, where water vapor is funneled toward it via the inward flux created by Knudsen diffusion. Another explanation for the discrepancy could be that thin film flow from the adsorbed water layer into the growing bridge takes place during growth: after a  $<2 \text{ nm}^3$  chain of water molecules is condensed, the negative Laplace pressure of the capillary bridge can start to attract already adsorbed water on the surfaces,<sup>29,33,48,55</sup> which in turn is replenished through Knudsen diffusion. However, water thin films are thought to be highly viscous,

which may slow down the water flow from the adsorbed layer into the capillary bridge.<sup>29,44</sup>

Once capillary nucleation and growth have taken place, the capillary bridge reaches a steady-state size. Interestingly, while the capillary bridge volume rises with separation, the capillary area, which is proportional to the adhesion force, decreases. This gap-adhesion dependency has also been shown by AFM pull-off experiments.<sup>48,56</sup> Furthermore, we find that at velocities in the range of  $10\text{--}100 \mu\text{m/s}$ , steady-state adhesion starts to decline with increasing velocity (Fig. 5). At greater tip-sample distances and, therefore, larger capillary bridge volumes, the decrease in steady-state adhesion as a function of velocity is observed at lower velocities than at intermediate or small tip-sample distances (smaller capillary bridge volume). Larger capillary bridges are more easily frustrated by lateral velocity. This finding is in quantitative agreement with contact mode adhesion measurements,<sup>33</sup> which were rescaled and included in Fig. 5.

#### IV. CONCLUSION

By repurposing the Lift Mode technique, we opened a new window into capillary condensation. The Lift Mode measurements provide the ability to measure the activation time for capillary condensation as a function of separation gap and lateral speed, as well as *in situ* observation of the growth of capillary bridges through measurement of adhesion force and quantification of the capillary bridge size and growth rate. We have benchmarked the Lift Mode method against other AFM studies<sup>33,35,42,47,48</sup> and found agreement for the distance-dependent activation time,<sup>42,47,52</sup> the velocity-dependent adhesion force,<sup>32,33</sup> and the growth of a liquid bridge.<sup>29,44</sup> The nucleation of capillary bridges is faster at smaller distances, in line with the thermal activation framework<sup>42,48</sup> and Knudsen diffusion at nanoscale interfaces.<sup>7,57</sup> In addition, we find a further increase in nucleation rate when applying a lateral velocity, possibly due to the enhancement of the Knudsen diffusion at the leading edge of the interface. Interestingly, the velocity-enhanced activation of capillary bridges may provide a physical mechanism behind the widely observed velocity strengthening friction in ambient systems.<sup>58</sup> Finally, we observe that the rate at which capillary bridges grow after nucleation is independent of the tip-sample distance and likely driven by the thin film flow of the nanometer-thick adsorbed water layer<sup>29,44</sup> in combination with a high adsorption rate of the growing water bridge to reach its thermal equilibrium. This observation highlights that Eqs. (1) and (2)—which are widely used in the literature to describe the thermally activated formation of capillary bridges of varying volumes—cannot capture the steady-state size of capillary bridges after growth.

Future studies can further investigate the influence of Knudsen diffusion on nucleation and growth dynamics by varying the interface geometry or adjusting environmental parameters, such as vapor pressure, surface chemistry, and temperature. Furthermore, the Lift Mode technique offers opportunities to study the interplay between capillary bridge growth and the thickness of pre-adsorbed water layers as well as the friction of confined water.<sup>30,59,60</sup> This opens new avenues to further understand the transport and exerted forces of water in confined interfaces in different fields of science, ranging from observed natural processes in biology<sup>1–3</sup> and geology<sup>5,10,58,61,62</sup> to friction- and adhesion-related engineering

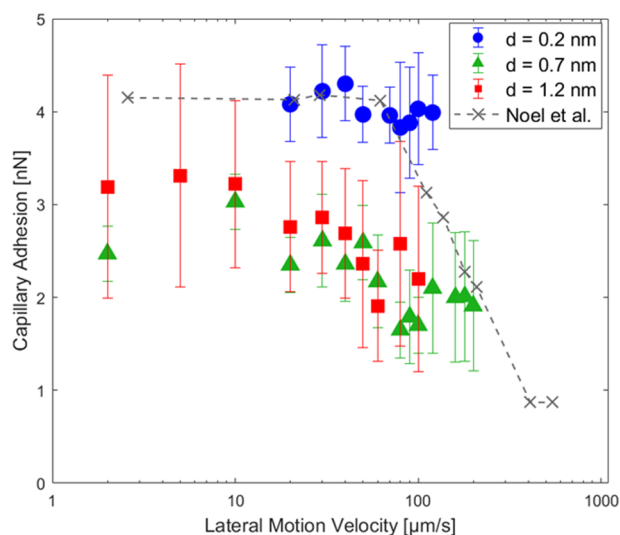


**FIG. 5.** Capillary adhesion forces at low lateral velocities are stable and show a dependence on tip-sample distance. With higher velocities, a reduction in adhesion force can be measured for tip-sample distances of 0.7 and 1.2 nm in a similar velocity regime as reported by Noel *et al.*<sup>33</sup> (gray dashed line, adhesion rescaled by factor 0.1).

challenges, such as nanometer-precise positioning systems in the semiconductor industry.<sup>63,64</sup>

## ACKNOWLEDGMENTS

We thank J. Brandon McClimon from the University of Pennsylvania for the thought-provoking discussions on capillary bridge formation and for the revision of the original manuscript.

## AUTHOR DECLARATIONS

### Conflict of Interest

The authors have no conflicts to disclose.

## Author Contributions

**Felix Cassin:** Conceptualization (lead); Data curation (lead); Formal analysis (equal); Investigation (lead); Methodology (lead); Visualization (lead); Writing – original draft (lead); Writing – review & editing (equal). **Rachid Hahury:** Formal analysis (supporting); Validation (equal); Writing – review & editing (equal). **Thibault Lançon:** Data curation (supporting); Formal analysis (supporting). **Steve Franklin:** Conceptualization (supporting); Supervision (supporting); Writing – review & editing (supporting). **Bart Weber:** Conceptualization (equal); Formal analysis (equal); Project administration (lead); Resources (lead); Supervision (lead); Validation (equal); Writing – review & editing (equal).

## DATA AVAILABILITY

The data that support the findings of this study are available from the corresponding author upon reasonable request.

## REFERENCES

- 1 R. Monson and D. Baldocchi, *Terrestrial Biosphere-Atmosphere Fluxes* (Cambridge University Press, New York, 2014).
- 2 R. L. CSIRO, "Transport of gases into leaves," *Plant, Cell Environ.* **6**, 181 (1983).
- 3 J. Armstrong and W. Armstrong, "A convective through-flow of gases in *Phragmites australis* (Cav.) Trin. ex Steud.," *Aquat. Bot.* **39**, 75 (1991).
- 4 W. Shi, R. M. Dalrymple, C. J. McKenny, D. S. Morrow, Z. T. Rashed, D. A. Surinach, and J. B. Boreyko, "Passive water ascent in a tall, scalable synthetic tree," *Sci. Rep.* **10**, 230 (2020).
- 5 Y. Wang, "Nanogeochemistry: Nanostructures, emergent properties and their control on geochemical reactions and mass transfers," *Chem. Geol.* **378-379**, 1 (2014).
- 6 Y. Liu, X. Zhou, D. Wang, C. Song, and J. Liu, "A diffusivity model for predicting VOC diffusion in porous building materials based on fractal theory," *J. Hazard. Mater.* **299**, 685 (2015).
- 7 H. Sun, J. Yao, D.-y. Fan, C.-c. Wang, and Z.-x. Sun, "Gas transport mode criteria in ultra-tight porous media," *Int. J. Heat Mass Transfer* **83**, 192 (2015).
- 8 G. Wen, S. Yang, Y. Liu, W. Wu, D. Sun, and K. Wang, "Influence of water soaking on swelling and microcharacteristics of coal," *Energy Sci. Eng.* **8**, 5 (2020).
- 9 D. Li, C. Xu, J. Y. Wang, and D. Lu, "Effect of Knudsen diffusion and Langmuir adsorption on pressure transient response in tight- and shale-gas reservoirs," *J. Pet. Sci. Eng.* **124**, 146 (2014).

- 10 T. L. Grove, C. B. Till, and M. J. Krawczynski, "The role of H<sub>2</sub>O in subduction zone magmatism," *Annu. Rev. Earth Planet. Sci.* **40**, 413 (2012).
- 11 E. Soylemez and M. P. De Boer, "Capillary-induced crack healing between surfaces of nanoscale roughness," *Langmuir* **30**, 11625 (2014).
- 12 F. W. DelRio, M. L. Dunn, L. M. Phinney, C. J. Bourdon, and M. P. De Boer, "Rough surface adhesion in the presence of capillary condensation," *Appl. Phys. Lett.* **90**, 163104 (2007).
- 13 D. Singh, H. Patel, A. Habal, A. K. Das, B. P. Kapgate, and K. Rajkumar, "Evolution of coefficient of friction between tire and pavement under wet conditions using surface free energy technique," *Constr. Build. Mater.* **204**, 105 (2019).
- 14 A. Fall, B. Weber, M. Pakpour, N. Lenoir, N. Shahidzadeh, J. Fiscina, C. Wagner, and D. Bonn, "Sliding friction on wet and dry sand," *Phys. Rev. Lett.* **112**, 175502 (2014).
- 15 J. Li, H. Chen, and H. A. Stone, "Ice lubrication for moving heavy stones to the Forbidden City in 15th- and 16th-century China," *Proc. Natl. Acad. Sci. U. S. A.* **110**, 20023 (2013).
- 16 C. A. Coulomb, *Theorie Des Machines Simple (Theory of Simple Machines)* (Bachelier, Paris, 1821).
- 17 C. A. Coulomb, "Essai sur une application des règles de maximis & minimis à quelques problèmes de statique, relatifs à l'architecture," in *Mémoires de Mathématique et de Physique, Présentés à l'Académie Royale des Sciences* (De l'Imprimerie Royale, 1773), pp. 343–382.
- 18 V. Popov, *History of Contact Mechanics and the Physics of Friction* (Springer Science and Business Media LLC, 2010).
- 19 E. Popova and V. L. Popov, "The legacy of Coulomb and generalized laws of friction," *PAMM* **20**, e202000062 (2021).
- 20 F. C. Hsia, S. Franklin, P. Audebert, A. M. Brouwer, D. Bonn, and B. Weber, "Rougher is more slippery: How adhesive friction decreases with increasing surface roughness due to the suppression of capillary adhesion," *Phys. Rev. Res.* **3**, 043204 (2021).
- 21 X. Xiao and L. Qian, "Investigation of humidity-dependent capillary force," *Langmuir* **16**, 8153 (2000).
- 22 F. C. Hsia, C. C. Hsu, L. Peng, F. M. Elam, C. Xiao, S. Franklin, D. Bonn, and B. Weber, "Contribution of capillary adhesion to friction at macroscopic solid-solid interfaces," *Phys. Rev. Appl.* **17**, 034034 (2022).
- 23 E. Riedo, I. Palaci, C. Boragno, and H. Brune, "The 2/3 power law dependence of capillary force on normal load in nanoscopic friction," *J. Phys. Chem. B* **108**, 5324 (2004).
- 24 A. Basu, G. G. Adams, and N. E. McGruer, "A review of micro-contact physics, materials, and failure mechanisms in direct-contact RF MEMS switches," *J. Micromech. Microeng.* **26**, 104004 (2016).
- 25 Z. Liu, J. Gong, C. Xiao, P. Shi, S. H. Kim, L. Chen, and L. Qian, "Temperature-dependent mechanochemical wear of silicon in water: The role of Si-OH surficial groups," *Langmuir* **35**, 7735 (2019).
- 26 S. Cheng and M. O. Robbins, "Capillary adhesion at the nanometer scale," *Phys. Rev. E* **89**, 062402 (2014).
- 27 Q. Yang, P. Z. Sun, L. Fumagalli, Y. V. Stebunov, S. J. Haigh, Z. W. Zhou, I. V. Grigorieva, F. C. Wang, and A. K. Geim, "Capillary condensation under atomic-scale confinement," *Nature* **588**, 250 (2020).
- 28 H.-J. Butt and M. Kappl, "Normal capillary forces," *Adv. Colloid Interface Sci.* **146**, 48 (2009).
- 29 Z. Wei and Y.-P. Zhao, "Growth of liquid bridge in AFM," *J. Phys. D: Appl. Phys.* **40**, 4368 (2007).
- 30 K. B. Jinesh and J. W. M. Frenken, "Capillary condensation in atomic scale friction: How water acts like a glue," *Phys. Rev. Lett.* **96**, 166103 (2006).
- 31 E. Riedo, F. Lévy, and H. Brune, "Kinetics of capillary condensation in nanoscopic sliding friction," *Phys. Rev. Lett.* **88**, 185505 (2002).
- 32 T. Lai, Y. Meng, W. Zhan, and P. Huang, "Logarithmic decrease of adhesion force with lateral dynamic revealed by an AFM cantilever at different humidities," *J. Adhes.* **94**, 334 (2018).
- 33 O. Noel, P. E. Mazeran, and H. Nasrallah, "Sliding velocity dependence of adhesion in a nanometer-sized contact," *Phys. Rev. Lett.* **108**, 015503 (2012).

- <sup>34</sup>M. W. Shin, T. H. Rhee, and H. Jang, "Nanoscale friction characteristics of a contact junction with a field-induced water meniscus," *Tribol. Lett.* **62**, 31 (2016).
- <sup>35</sup>M. V. Vitorino, A. Vieira, C. A. Marques, and M. S. Rodrigues, "Direct measurement of the capillary condensation time of a water nanobridge," *Sci. Rep.* **8**, 13848 (2018).
- <sup>36</sup>P.-E. Mazeran, "Effect of sliding velocity on capillary condensation and friction force in a nanoscopic contact," *Mater. Sci. Eng. C* **26**, 751 (2006).
- <sup>37</sup>T. Lai, Y. Meng, H. Tang, and G. Yu, "Influence of lateral velocity on adhesion force of surfaces with different hydrophilicity revealed by an AFM colloidal probe at humid environments," *J. Adhes.* **94**, 1036 (2018).
- <sup>38</sup>Y. I. Rabinovich, J. J. Adler, M. S. Esayanur, A. Ata, R. K. Singh, and B. M. Moudgil, "Capillary forces between surfaces with nanoscale roughness," *Adv. Colloid Interface Sci.* **96**, 213 (2002).
- <sup>39</sup>L. Xu, A. Lio, J. Hu, D. F. Ogletree, and M. Salmeron, "Wetting and capillary phenomena of water on mica," *J. Phys. Chem. B* **102**, 540 (1998).
- <sup>40</sup>Y. Men, X. Zhang, and W. Wang, "Capillary liquid bridges in atomic force microscopy: Formation, rupture, and hysteresis," *J. Chem. Phys.* **131**, 184702 (2009).
- <sup>41</sup>D. B. Asay and S. H. Kim, "Effects of adsorbed water layer structure on adhesion force of silicon oxide nanoasperity contact in humid ambient," *J. Chem. Phys.* **124**, 174712 (2006).
- <sup>42</sup>R. Szoszkiewicz and E. Riedo, "Nucleation time of nanoscale water bridges," *Phys. Rev. Lett.* **95**, 135502 (2005).
- <sup>43</sup>S. H. Yang, M. Nosonovsky, H. Zhang, and K.-H. Chung, "Nanoscale water capillary bridges under deeply negative pressure," *Chem. Phys. Lett.* **451**, 88 (2008).
- <sup>44</sup>L. Sirghi, "Transport mechanisms in capillary condensation of water at a single-asperity nanoscopic contact," *Langmuir* **28**, 2558 (2012).
- <sup>45</sup>A. Berman, C. Drummond, and J. Israelachvili, "Amontons' law at the molecular level," *Tribol. Lett.* **4**, 95 (1998).
- <sup>46</sup>C. Greiner, J. R. Felts, Z. Dai, W. P. King, and R. W. Carpick, "Controlling nanoscale friction through the competition between capillary adsorption and thermally activated sliding," *ACS Nano* **6**, 4305 (2012).
- <sup>47</sup>B. Sung, J. Kim, C. Stambaugh, S. J. Chang, and W. Jhe, "Direct measurement of activation time and nucleation rate in capillary-condensed water nanomeniscus," *Appl. Phys. Lett.* **103**, 213107 (2013).
- <sup>48</sup>L. Sirghi, R. Szoszkiewicz, and E. Riedo, "Volume of a nanoscale water bridge," *Langmuir* **22**, 1093 (2006).
- <sup>49</sup>E. Soylemez and M. P. De Boer, "Modeling capillary bridge dynamics and crack healing between surfaces of nanoscale roughness," *J. Micromech. Microeng.* **27**, 125023 (2017).
- <sup>50</sup>C. Xiao, F. Elam, S. Van Vliet, R. Bliem, S. Lepany, N. Shahidzadeh, B. Weber, and S. Franklin, "Intercrystallite boundaries dominate the electrochemical corrosion behavior of polycrystalline diamond," *Carbon* **200**, 1 (2022).
- <sup>51</sup>V. G. Gisbert, C. A. Amo, M. Jaafar, A. Asenjo, and R. Garcia, "Quantitative mapping of magnetic properties at the nanoscale with bimodal AFM," *Nanoscale* **13**, 2026 (2021).
- <sup>52</sup>M. V. Vitorino, A. Vieira, C. A. Marques, and M. S. Rodrigues, "Direct measurement of the capillary condensation time of a water nanobridge," *Sci. Rep.* **8**, 13848 (2018).
- <sup>53</sup>S. Varoutis, S. Naris, V. Hauer, C. Day, and D. Valougeorgis, "Computational and experimental study of gas flows through long channels of various cross sections in the whole range of the Knudsen number," *J. Vac. Sci. Technol. A* **27**, 89 (2009).
- <sup>54</sup>F. Colson and D. A. Barlow, "Statistical method for modeling Knudsen diffusion in nanopores," *Phys. Rev. E* **100**, 062125 (2019).
- <sup>55</sup>Z. Wei, Y. Sun, W. X. Ding, and Z. R. Wang, "The formation of liquid bridge in different operating modes of AFM," *Sci. China: Phys., Mech. Astron.* **59**, 694611 (2016).
- <sup>56</sup>G. Mason and W. C. Clark, "Liquid bridges between spheres," *Chem. Eng. Sci.* **20**, 859 (1965).
- <sup>57</sup>W. Szmyt, C. Guerra-Nuñez, C. Dransfeld, and I. Utke, "Solving the inverse Knudsen problem: Gas diffusion in random fibrous media," *J. Membr. Sci.* **620**, 118728 (2021).
- <sup>58</sup>Y. Bar-Sinai, R. Spatschek, E. A. Brener, and E. Bouchbinder, "On the velocity-strengthening behavior of dry friction," *J. Geophys. Res.: Solid Earth* **119**, 1738, <https://doi.org/10.1002/2013JB010586> (2014).
- <sup>59</sup>M. Lee, H. Choi, B. Kim, and J. Kim, "Giant fluidic impedance of nanometer-sized water bridges: Shear capillary force at the nanoscale," *Phys. Rev. E* **105**, 065108 (2022).
- <sup>60</sup>I. Barel, A. E. Filippov, and M. Urbakh, "Formation and rupture of capillary bridges in atomic scale friction," *J. Chem. Phys.* **137**, 164706 (2012).
- <sup>61</sup>L. Chen and L. Qian, "Role of interfacial water in adhesion, friction, and wear—A critical review," *Friction* **9**, 1 (2021).
- <sup>62</sup>J. M. Sharp, Jr. and J. R. Kyle, "The role of ground-water processes in the formation of ore deposits," in *Hydrogeology*, edited by W. Back, J. S. Rosenshein, and Paul R. Seaber (1988).
- <sup>63</sup>H. Mishina and A. Hase, "Effect of the adhesion force on the equation of adhesive wear and the generation process of wear elements in adhesive wear of metals," *Wear* **432-433**, 202936 (2019).
- <sup>64</sup>C. M. Mate, "Application of disjoining and capillary pressure to liquid lubricant films in magnetic recording," *J. Appl. Phys.* **72**, 3084 (1992).
- <sup>65</sup>O. Noël, P. E. Mazeran and I. Stanković, "Nature of dynamic friction in a humid hydrophobic nanocontact," *ACS Nano*, **16**(7), 10768–10774 (2022).